Rare-gas solids under pressure: A path-integral Monte Carlo simulation

Carlos P. Herrero and Rafael Ramírez
Instituto de Ciencia de Materiales, Consejo Superior de Investigaciones Científicas (CSIC), Campus de Cantoblanco, 28049 Madrid, Spain

(Received 16 September 2004; revised manuscript received 10 December 2004; published 25 May 2005)

Rare-gas solids (Ne, Ar, Kr, and Xe) under hydrostatic pressure up to 30 kbar have been studied by path-integral Monte Carlo (PIMC) simulations in the isothermal-isobaric ensemble. Results of these simulations have been compared with available experimental data and with those obtained from a quasiharmonic approximation (QHA). This comparison allows us to quantify the overall anharmonicity of the lattice vibrations and its influence on several structural and thermodynamic properties of rare-gas solids. The vibrational energy increases with pressure, but this increase is slower than that of the elastic energy, which dominates at high pressures. In the PIMC simulations, the vibrational kinetic energy is found to be larger than the corresponding potential energy, and the relative difference between both energies decreases as the applied pressure is raised. The accuracy of the QHA increases for rising pressure.

DOI: 10.1103/PhysRevB.71.174111 PACS number(s): 67.80.−s, 62.50.+p, 65.40.De, 05.10.Ln

I. INTRODUCTION

The importance of anharmonic effects in solids has been recognized long ago, as they are responsible for well-known phenomena such as thermal expansion, pressure dependence of the compressibility, phonon couplings, as well as isotope dependence of structural properties and melting temperature.[1,2] These kinds of effects have been studied both theoretically and experimentally for rare-gas solids for many years[3,4] because these are simple systems allowing fruitful comparisons between theory and experiment. The interatomic forces are weak, short range, and rather well understood, so critical tests of appropriate theories by their ability to predict properties of actual rare-gas crystals are relatively simple. In particular, their thermodynamic properties are interesting due to the large anharmonic contributions to their lattice dynamics.

From a theoretical point of view, anharmonic effects in solids have been traditionally studied by using approaches such as the so-called quasiharmonic approximation (QHA).[1,2] In this approach, frequencies of vibrational modes are assumed to change with crystal volume, and for given volume and temperature, the solid is supposed to be harmonic.[5,6] However, the QHA does not deal with phonon interaction effects, which can be treated by perturbation theory[7] when anharmonicity is not large, or by different self-consistent phonon theories for larger anharmonicities.[8–11] A different theoretical procedure is the Feynman path integral method,[12] which is well suited to study thermodynamic properties of solids at temperatures lower than the Debye temperature Θ_D, where the quantum nature of the atomic nuclei is relevant. The combination of path integrals with Monte Carlo (MC) sampling enables us to carry out quantitative and nonperturbative studies of anharmonic effects in solids. The path-integral Monte Carlo (PIMC) technique has been applied earlier to study several properties of rare-gas solids.[13–19] In particular, it has predicted kinetic-energy values in good agreement with experimental data.[20,21] An effective-potential Monte Carlo theory[22,23] has also been applied to study thermal and elastic properties of solid neon.

Anharmonic effects increase appreciably with temperature. This is now well known and has been explained quantitatively for rare-gas solids.[5,22] In recent years, the effect of pressure on these solids has attracted much attention from both experimentalists[24–27] and theorists.[6,14,28,29] The influence of pressure on the anharmonicity of lattice vibrations is, however, not well understood. It has been recently suggested that pressure causes a decrease in this anharmonicity,[30,31] in line with earlier observations that the accuracy of the QHA increases as pressure is raised.[32] It has also been argued that at high pressures, thermodynamic properties of solids can be well described by classical calculations, i.e., dealing with the atoms as classical oscillators in a given potential.[33] This seems to be, at first sight, contradictory with the fact that pressure induces a larger zero-point vibrational energy of the solid. These questions are indeed related to the ratio of the vibrational energy to the whole internal energy on one side, and to the size of the "intrinsic" anharmonicity (further than the QHA) of the lattice vibrations on the other side.

In this paper, we study structural and thermodynamic properties of rare-gas solids under pressure. This allows us to study properties of these solids along well-defined isotherms, and to analyze changes in anharmonic effects due to the repulsive (for compression) and attractive (for dilation, i.e., negative pressure) parts of the interatomic potential. The interatomic interaction is described by a Lennard-Jones potential. Results of the PIMC simulations are compared with those yielded by a quasiharmonic approximation with the same interatomic potential. This approach will help us to quantify the influence of the "intrinsic" anharmonicity on the considered properties.

The paper is organized as follows. In Sec. II, the computational method is described. In Sec. III, we present results for energy, heat capacity, lattice parameter, and bulk modulus. Finally, Sec. IV includes a discussion of the results and the conclusions.

TABLE I. Parameters σ and ϵ of the Lennard-Jones potential employed in this work and average isotopic mass $\langle M \rangle$ for rare gases. Calculated zero-temperature properties of rare-gas solids at zero pressure are also given: lattice parameter a, zero-point vibrational energy E_{vib}, and elastic energy E_{el} per atom, as derived from PIMC simulations.

Element	σ (Å)	ϵ (meV)	$\langle M \rangle$ (amu)	a (Å)	E_{vib} (meV)	E_{el} (meV)
Ne	2.782	3.084	20.18	4.4631	6.33	1.20
Ar	3.404	10.32	39.95	5.3115	7.99	0.43
Kr	3.638	14.17	83.80	5.6458	6.27	0.18
Xe	3.961	19.91	131.30	6.1316	5.54	0.10

II. METHOD

A. Path-integral Monte Carlo

Rare-gas atoms were treated as quantum particles interacting through a Lennard-Jones potential: $V(r)=4\epsilon[(\sigma/r)^{12}-(\sigma/r)^6]$, with parameters ϵ and σ given in Table I, which were employed in earlier simulations of these kinds of crystals.[18,19] In this table we also give the average atomic mass of rare gases used in the calculations, as well as low-temperature properties of the studied crystals at zero pressure, as derived from PIMC simulations (see below). Lennard-Jones-type potentials have been employed in recent years to model the atomic interaction in rare-gas solids.[16,17,22,23] Although more sophisticated interaction potentials have been developed, they do not seem to be significantly superior to Lennard-Jones potentials in accounting for the experimental data.[16,22] This is not the case when one considers rare-gas solids under high pressure, where three-body potentials are necessary (see below). For this reason, our calculations are restricted to pressures not higher than 30 kbar.

Equilibrium properties of rare-gas solids have been calculated by PIMC simulations in the isothermal-isobaric ensemble (NPT). Simulations have been performed on $5\times5\times5$ cubic supercells of the face-centered-cubic unit cell, including 500 rare-gas atoms, and assuming periodic boundary conditions. To check the convergence of our results with system size, some MC simulations were carried out for other supercell sizes, including $7\times7\times7$ supercells. We found that finite-size effects for $5\times5\times5$ supercells are negligible for the quantities studied here (they are smaller than the statistical noise).

In the path-integral formulation of statistical mechanics, the partition function is evaluated through a discretization of the density matrix along cyclic paths, composed of a finite number N_{Tr} (Trotter number) of "imaginary-time" steps.[12] In the numerical simulations, this discretization gives rise to the appearance of N_{Tr} replicas for each quantum particle. In this way, the implementation of this method is based on an isomorphism between the quantum system and a classical one, obtained by replacing each quantum particle (here, atomic nucleus) by a cyclic chain of N_{Tr} classical particles, connected by harmonic springs with a temperature-dependent constant. Details on this computational method can be found elsewhere.[34–36]

To have a nearly constant precision for the simulation results at different temperatures, we considered a Trotter number that scales as the inverse temperature. At a given T, the actual value N_{Tr} required to obtain convergence of the results depends on the Debye temperature Θ_D (higher Θ_D needs larger N_{Tr}). For the simulations at zero pressure, we have taken $N_{\mathrm{Tr}}T=250$ K for solid Ar and $N_{\mathrm{Tr}}T=200$ K for the other rare-gas solids ($\Theta_D\sim90$ K for Ar versus ~70 K for Ne, Kr, and Xe). Since vibrational frequencies (and the associated Debye temperature) increase as the applied pressure is raised, the Trotter number has to be correspondingly increased. Thus, for a given solid and an applied pressure we have taken N_{Tr} values roughly proportional to the zero-point vibrational energy at the considered pressure. This means that N_{Tr} is increased by a factor of about 2 for Ar, Kr, and Xe (about three for Ne) when pressure rises from zero to 30 kbar. Thus, the computational time required to carry out PIMC simulations rises (a) as temperature is lowered ($\propto 1/T$) and (b) as pressure is raised [$\propto E_{\mathrm{vib}}(0)$, zero-point vibrational energy]. For example, a PIMC simulation for solid Ar at 5 K and zero pressure ($N_{\mathrm{Tr}}=50$, $N=500$) is equivalent in computational time to a classical MC simulation for $N_{\mathrm{Tr}}N=25\,000$ atoms. This number increases by a factor of 2 at the same temperature and $P=30$ kbar.

Sampling of the configuration space has been carried out by the Metropolis method at temperatures between 5 K and the triple-point temperature T_{tp} of the different solids, as well as at pressures up to 30 kbar. For given temperature and pressure, a typical run consisted of the generation of 2×10^4 quantum paths per atom for system equilibration, followed by 3×10^5 paths per atom for the calculation of ensemble average properties. Other technical details are the same as those used in Refs. 18 and 19.

The isothermal bulk modulus B can be obtained in the NPT ensemble from the mean-square fluctuations in the lattice parameter, σ_a^2. In this ensemble, fluctuations in the volume V of the simulation cell are given by[37] $\sigma_V^2=Vk_BT/B$, and therefore

$$B=\frac{k_BT}{9L^3a\sigma_a^2}, \tag{1}$$

where L is the side length of the simulation cell in units of the lattice parameter (here, $L=5$).

B. Quasiharmonic approximation

In the following section, results of PIMC simulations are compared with those derived from a QHA. This approxima-

tion is based on a renormalization of the phonon frequencies with volume, and for a given volume the solid is assumed to be harmonic.[1,2] This volume dependence of phonon frequencies is usually described by a mode-dependent Grüneisen parameter[1,2] $\gamma_n(\mathbf{q}) = -\partial \ln \omega_n(\mathbf{q}) / \partial \ln V$, where $\omega_n(\mathbf{q})$ are the frequencies of the nth mode in the crystal, and for small volume changes $\gamma_n(\mathbf{q})$ is assumed to be constant for each mode. However, for the QHA calculations presented here, we have not employed this description based on Grüneisen parameters. Instead of this, we calculate directly the actual (harmonic) vibrational frequencies for each crystal volume by diagonalizing the corresponding dynamical matrix.

For direct comparison with results of PIMC simulations, we have employed for the QHA the same supercell as for the simulations, i.e., a $5\times5\times5$ supercell with periodic boundary conditions. This means that only the $\mathbf{q}=0$ modes in the Brillouin zone of the supercell are included in the calculation, since modes with $\mathbf{q}\neq 0$ violate the periodic boundary conditions. Then, the total number of vibrational modes in the QHA is 1497, i.e., three times the number of rare-gas atoms in the supercell minus three translational degrees of freedom. The point group symmetry of the simulation cell imposes that many of these normal frequencies are degenerated. The number of normal modes that are not symmetry equivalent is 72 for the supercell employed here. For each temperature, we calculated the free energy as a function of volume, with the corresponding phonon frequencies. The lattice parameter was changed in steps of 10^{-3} Å, and from the volume derivative of the free energy we derived the equilibrium volume as a function of pressure.

III. RESULTS

A. Energy

Once defined an interatomic potential, the internal energy of a solid, $E(V,T)$, at given volume and temperature can be written as

$$E(V,T) = E_0 + E_{\mathrm{el}}(V) + E_{\mathrm{vib}}(V,T), \tag{2}$$

where E_0 is the minimum potential energy for the (classical) crystal at $T=0$, $E_{\mathrm{el}}(V)$ is the elastic energy, and $E_{\mathrm{vib}}(V,T)$ is the vibrational energy. Since we are working in the isothermal-isobaric ensemble, it is understood that the volume is implicitly given by the applied pressure, i.e., $V=V(P)$. For a given volume V, the classical energy at $T=0$ increases by an amount $E_{\mathrm{el}}(V)$ with respect to the minimum energy E_0. This elastic energy E_{el} depends only on volume, but at finite temperatures and for the real (quantum) solids, it depends implicitly on T due to the temperature dependence of V (thermal expansion). The elastic energy $E_{\mathrm{el}}(V)$ represents a nonnegligible part of the internal energy, even at zero pressure. For example, in Ne it is found to be 1.2 and 2.1 meV per atom at 5 and 24 K, respectively. These values are smaller for the other rare gases, as shown in Table I.

The vibrational energy, $E_{\mathrm{vib}}(V,T)$, depends explicitly on both, V and T, and can be obtained by subtracting the elastic energy from the internal energy. Values of E_{vib} derived from our PIMC simulations for $T\to 0$ and $P=0$ are given in Table

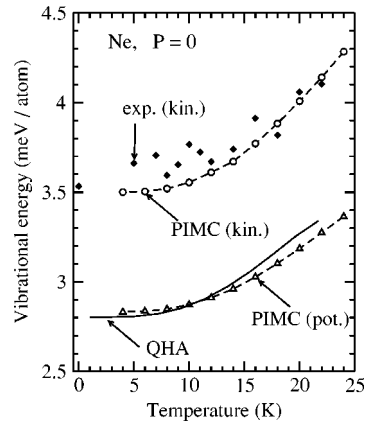

FIG. 1. The temperature dependence of the vibrational energy of solid neon. Circles and triangles correspond to kinetic and potential energy, respectively, as derived from PIMC simulations. Error bars of the simulation results are less than the symbol size. Dashed lines are guides to the eye. The solid line is the result of the QHA. Diamonds are kinetic-energy data for solid Ne, obtained by Timms *et al.* (Ref. 20) from neutron Compton scattering (the point at $T=0$ is an extrapolation given by these authors).

I. Path-integral Monte Carlo simulations allow us to obtain separately the kinetic energy, E_k, and potential energy, E_p, associated to the lattice vibrations.[34] Both energies are shown in Fig. 1 for solid Ne as a function of temperature at $P=0$. Circles and triangles correspond to the vibrational kinetic and potential energy, respectively. Our results for the kinetic energy are close to those derived earlier from PIMC simulations with Lennard-Jones[13,21,38] and Aziz[38] interatomic potentials. For comparison, we present also in Fig. 1 values of the kinetic energy of Ne atoms, derived by Timms *et al.*[20] from neutron Compton scattering in solid neon (black diamonds). According to the results of our PIMC simulations, E_k is larger than E_p by about 20%. The QHA predicts potential (and kinetic) energy values (solid line) that are close to the vibrational potential energy derived from our PIMC simulations. Something similar happens for the other rare-gas solids, with $E_k > E_p$ for all temperatures and pressures studied here. The difference $E_k - E_p$ decreases for increasing atomic mass, and at $T=5$ K and zero pressure, we find $E_k - E_p = 0.67$ and 0.059 meV/atom for Ne and Xe, respectively. These energy differences increase slowly as pressure rises, and take values of 0.75 and 0.060 meV/atom for Ne and Xe at 30 kbar.

A quantitative estimation of the overall anharmonicity of the atom vibrations is given by the parameter[17] $\xi = 2(E_k - E_p)/(E_k + E_p)$, which should be zero for a harmonic solid at any temperature, as follows from the virial theorem. For rare-gas solids, it was shown earlier[19] that ξ increases as temperature rises, as expected for larger anharmonicity. In Fig. 2 we show the pressure dependence of the parameter ξ for different rare-gas solids at $T=5$ K, as derived from PIMC simulations. One observes that ξ decreases as pressure is raised. The relative change in this parameter is largest for Ne, for which it decreases by a factor of about 3.5. For Xe, it changes by a factor ≈ 2.

The elastic energy E_{el} increases fast as pressure rises. In Fig. 3 we display the pressure dependence of E_{el} for (a) Ne

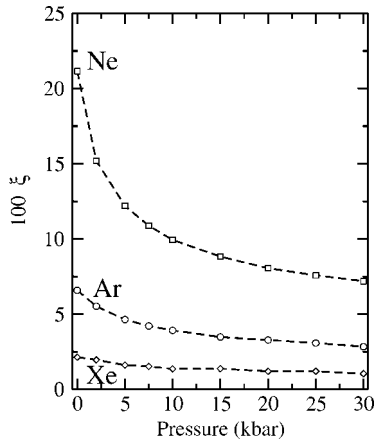

FIG. 2. The anharmonicity parameter ξ for rare-gas crystals as a function of applied hydrostatic pressure. Symbols indicate results of PIMC simulations at $T=5$ K. From top to bottom: Ne, Ar, and Xe. Error bars are less than the symbol size. Lines are guides to the eye. Results for Kr lie between those for Ar and Xe and are not shown for clarity of the figure.

and (b) Ar, obtained from PIMC (open squares) and QHA (solid lines). For comparison we also present results for the vibrational energy (kinetic plus potential) obtained by both procedures. As shown above, E_k for Ne at zero pressure is about 20% larger than E_p, and thus the whole $E_{\rm vib}$ derived from PIMC is 10% larger than that found in the QHA (E_p is nearly the same for both methods). This relative difference decreases as pressure increases, and is almost inobservable on the scale of Fig. 3. Note that close to $P=0$, $E_{\rm el}$ decreases as P rises, reaches a minimum, and then increases continuously for larger applied pressures. This is due to the fact that at $P=0$ the crystal is expanded with respect to the volume giving the minimum potential energy. With an applied pressure of about 2 kbar, solid neon reaches the volume corresponding to the classical minimum (giving $E_{\rm el}=0$), and for larger pressures the volume is further reduced, with an increase in $E_{\rm el}$. Something similar happens for Ar and the other rare-gas solids, although it is less appreciable on the scale of Fig. 3(b). For solid Ne we find that the vibrational energy is larger than $E_{\rm el}$ at pressures $P<23$ kbar. However, $E_{\rm el}$ rises faster with pressure, and becomes the dominant part of the internal energy for larger pressures. This behavior is qualitatively similar for the other rare-gas solids, as shown in Fig. 3(b) for Ar. The main difference is that the elastic energy for Ar increases with pressure faster than for Ne, and becomes larger than $E_{\rm vib}$ for $P>12$ kbar. In this context, the main point concerning large pressures is that $dE_{\rm el}/dP>dE_{\rm vib}/dP$. This means that the ratio $E_{\rm el}/E_{\rm vib}$ grows for increasing pressure, and eventually the vibrational energy becomes a small correction to the internal energy.

Note that in Fig. 3 we have included some points at negative pressure (that is, solids under tension). This region with $P<0$ was studied earlier for rare-gas solids by PIMC simulations.[39] It was found, in particular, that at $T=5$ K solid Ne and Ar are metastable until reaching the corresponding spinodal pressures of -0.9 and -2.5 kbar, where they become mechanically unstable. Here we only comment that energy results obtained from the QHA follow those yielded by PIMC simulations also in this region of negative pressures.

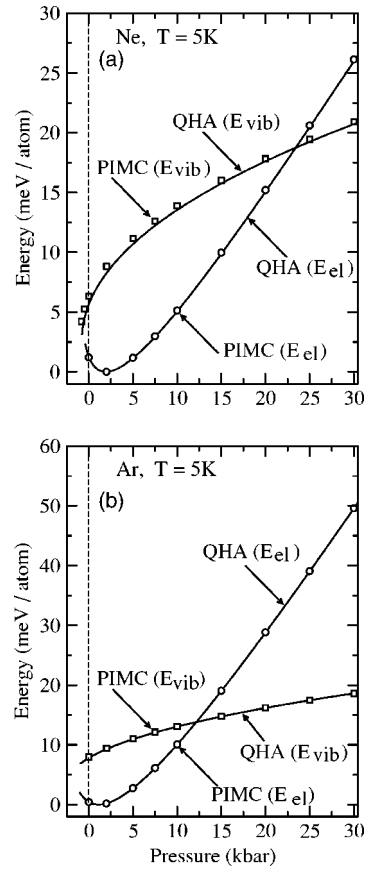

FIG. 3. The vibrational and elastic energy of solid Ne (a) and Ar (b) at $T=5$ K, as a function of pressure. Symbols show results of PIMC simulations: □: vibrational energy; ○: elastic energy. Solid lines are results of the quasiharmonic approximation. The error bars of the simulation results are less than the symbol size.

B. Heat capacity

We have calculated the heat capacity C_p of rare-gas solids for several pressures as a numerical derivative of the enthalpy, $H=E+PV$, with respect to the temperature. In Fig. 4 we present results derived from PIMC simulations (symbols) for solid argon at $P=0$ and 15 kbar. Results of the quasiharmonic approximation are shown as dashed lines. For comparison, we also present experimental results obtained by Flubacher *et al.*[40] for argon at atmospheric pressure. Results of PIMC simulations at $P=0$ agree well with experimental data for both Ne and Ar (data for Ne were given elsewhere[18] and are not shown here), except close to $T_{\rm tp}$, where the simulation results are lower than the experimental ones in both cases. However, for $T\lesssim T_{\rm tp}$ there can be a systematic error in the experimental results ($\sim$10% at $T_{\rm tp}$), due to partial vaporizing of the solid.[41] Our simulations were carried out for perfect crystals (without vacancies), and thus we cannot conclude at this point if the observed difference is caused by a failure of the Lennard-Jones potential employed here, or by the experimental uncertainty near $T_{\rm tp}$.

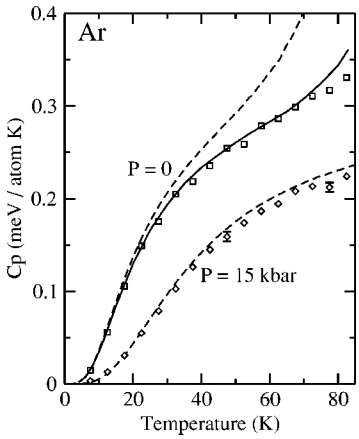

FIG. 4. The heat capacity, C_p, of solid argon as a function of temperature at $P=0$ and 15 kbar. Symbols: PIMC simulations; dashed lines: quasiharmonic approximation; solid line: experimental data obtained by Flubacher *et al.* (Ref. 40) at atmospheric pressure. The error bars of the simulation results for $P=0$ are on the order of the symbol size.

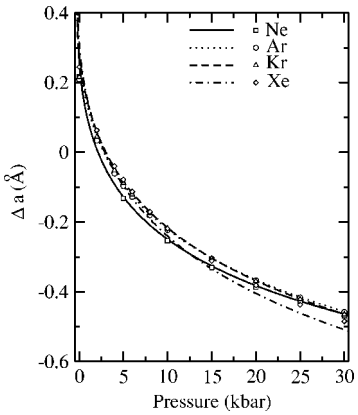

FIG. 5. The pressure dependence of the increment in lattice parameter, $\Delta a = a - a_{cl}(0)$, with respect to the ideal (classical) crystal with minimum potential energy. Symbols and lines indicate results of PIMC simulations and QHA along a given isotherm for each solid: Ne at 20 K (□, solid line), Ar at 80 K (○, dotted line), Kr at 110 K (△, dashed line), and Xe at 160 K (◇, dashed-dotted line).

For zero pressure, the QHA gives results close to those of PIMC at low temperatures ($T<5$ K for Ne and $T<20$ K for Ar), but clearly overestimates the heat capacity at higher temperatures. The relative error of the QHA (compared with PIMC) increases as temperature is raised, as expected for an increase in (intrinsic) anharmonicity due to thermal effects. In the case of Ne, this approximation breaks down at $T=22.6$ K, due to a mechanical instability (the solid becomes unstable in the QHA at a temperature lower than the actual T_{tp}). For Ar this approach predicts a breakdown of the solid at 86.2 K. These results are in line with earlier observations on the validity temperature range of the QHA for these solids[4,5,42]

For increasing pressure, the error of the QHA decreases. This is in part due to the renormalization of vibrational frequencies, which increase under an applied pressure, and therefore shift the increase in C_p to higher temperatures. Moreover, the relative contribution of the vibrational energy to the internal energy is reduced as pressure rises, and in consequence the intrinsic anharmonicity of the vibrational modes (not captured by the QHA) becomes less relevant for the heat capacity.

C. Lattice parameter

At $T=0$, the difference $\Delta a(0)=a(0)-a_{cl}(0)$ between the actual lattice parameter $a(0)$ and that corresponding to the minimum potential energy of the (classical) crystal, $a_{cl}(0)$, decreases as the atomic mass rises and quantum effects become less relevant.[17,43] From our PIMC simulations we found at $P=0$ that $\Delta a(0)$ ranges from 0.174 Å for Ne to 0.025 Å for Xe. Calculated values for $a(0)$ at zero pressure are given in Table I. The temperature dependence of the lattice parameter derived from this kind of PIMC simulation agrees with experimental data for rare-gas solids.[18,19] Such an agreement is also found at low temperatures in the pressure range considered here ($P\leqslant 30$ kbar). In this pressure range, the QHA predicts lattice parameters that follow closely those given by the simulations (see below the discussion on the bulk modulus).

For large pressures, it is known that the description of rare-gas solids with effective interatomic potentials requires the consideration of three-body terms[14,24,44] to reproduce the actual equation of state *P-V*. We have checked that the Lennard-Jones potential considered here predicts *P-V* isotherms for solid Ar close to the experimental ones[26] up to pressures on the order of 50 kbar. For larger pressures, this pair potential yields volumes larger than the real ones.

Even though thermal effects on the crystal volume change in magnitude for different rare-gas solids at low temperatures ($T\lesssim 5$ K), these differences are less important at higher temperatures. If one takes as a reference the classical lattice parameter $a_{cl}(0)$, the difference $\Delta a=a-a_{cl}(0)$ at temperatures close to T_{tp} of each solid amounts to ≈ 0.25 Å, as derived from our PIMC simulations. This difference Δa is plotted in Fig. 5 for the different solids as a function of pressure. For each solid we present PIMC results along an isotherm: Ne, $T=20$ K; Ar, 80 K; Kr, 110 K; and Xe, 160 K. These results for the different rare-gas solids follow roughly the same pressure dependence. Note that at $P=0$, Δa is positive, as a consequence of zero-point and thermal lattice expansion. Under applied pressure Δa decreases, reaching $\Delta a=0$ for a pressure $P\approx 2$ kbar, and is negative for larger P. Lines in this figure show results of the QHA, which follow closely those of PIMC. The main difference between both sets of results appears for Xe at pressures higher than 10 kbar (diamonds and dashed-dotted lines). We conclude that the difference Δa at temperatures near T_{tp} follows a pressure dependence similar for all rare-gas solids considered here.

D. Bulk modulus

The isothermal bulk modulus B of rare-gas solids has been calculated from our PIMC simulations by using Eq. (1). The temperature dependence of B at zero pressure was stud-

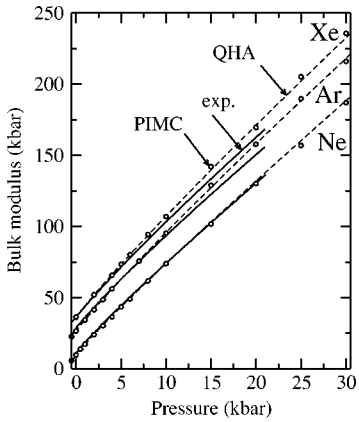

FIG. 6. The isothermal bulk modulus as a function of pressure for rare-gas solids. Symbols: results of PIMC simulations at $T=5$ K, with error bars on the order of the symbol size. Dashed lines: quasiharmonic approximation at 5 K. Solid lines: experimental data by Anderson *et al.* (Ref. 46) for Ne, and Anderson and Swenson (Ref. 47) for Ar and Xe, at $T=4.2$ K.

ied earlier[18,19] and will not be presented here. We only note that results obtained from this kind of simulations for Ar, Kr, and Xe showed good agreement with experimental data up to temperatures close to T_{tp}.[18,19] Results found for the bulk modulus of neon are lower than the experimental data at $T<18$ K, and at higher T the experimental B decreases faster than that derived from the simulations. This seems to be a general problem of this kind of calculation with Lennard-Jones- and Tang-Toennis-type interatomic potentials.[22,45]

We now turn to the pressure dependence of the bulk modulus for these solids. Results of our PIMC simulations for Ne, Ar, and Xe at $T=5$ K are plotted in Fig. 6 (symbols). The bulk modulus of Kr (not shown for clarity) lies between those of Ar and Xe. Dashed lines are results of the QHA, and solid lines represent experimental data obtained by Anderson *et al.*[46] for Ne and Anderson and Swenson[47] for Ar and Xe. The QHA predicts bulk moduli in good agreement with those derived from PIMC simulations, indicating that this approximation is rather accurate for predicting the P-V equation of state, as well as the derivative $\partial P/\partial V$, which gives the bulk modulus.

Our calculated results for Ne agree well with experimental data in the pressure region under consideration. For the other rare-gas solids (including Kr, not shown in Fig. 6) our results are larger than the experimental data for $P \gtrsim 10$ kbar. At 20 kbar, our method overestimates the bulk modulus of Ar and Xe by about 5%. This is a consequence of the interatomic pair potential employed in our calculations. As indicated above, the limitation of pair potentials for describing this kind of solid shows up as pressure rises, and eventually three-body terms are necessary at high pressures.[14,44]

IV. DISCUSSION

Path-integral Monte Carlo simulations give in principle the "exact" solution to the considered quantum problem, with an accuracy depending on the considered Trotter number and the statistical error associated to the MC sampling. Thus, the Lennard-Jones potential employed here gives a good description of structural and thermodynamic properties of rare-gas solids at zero pressure between $T=0$ and the triple-point temperature. The equation of state P-V is well described by this potential in the pressure range considered here ($P<30$ kbar). The bulk modulus of Ne is well reproduced, and for heavier rare gases PIMC simulations give B values larger than experiment at $P \gtrsim 10$ kbar.

In all solids considered here, and for different pressures and temperatures, we have found $E_k > E_p$. The overall anharmonicity has been measured by the parameter ξ, which for given T and P decreases as the atomic mass is raised. Although this parameter is by no means a unique and absolute measure of the whole anharmonicity, for a family of similar materials it is useful to give us a quantitative estimation of anharmonic effects as a function of atomic mass, temperature, and pressure. In the limit $P=0$ and $T \to 0$, ξ changes from 0.21 for Ne to 0.02 for Xe. This indicates a large anharmonicity of the lattice vibrations in Ne, even at $T=0$. For comparison, we note that covalent solids at low temperatures show much lower values of ξ. Thus, for diamond, silicon, and germanium one finds, for $T/\Theta_D \ll 1$, differences between E_p and E_k smaller than 1%, and at $T \sim \Theta_D$ they are less than 3%.[43,48,49] Another point of interest is that for such covalent materials the vibrational E_p was found to be larger than E_k, just the opposite to the trend found for rare-gas solids. Then, the fact that $E_p < E_k$, obtained for the rare-gas solids studied here, is not general in solids, and can be due to the particular nature of the interatomic interactions present in rare-gas (Lennard-Jones) solids.

A qualitative understanding of the sizeable increase in kinetic energy of the rare-gas atoms with respect to the value expected in a QHA can be obtained by analyzing the changes of kinetic and potential energy by standard time-independent perturbation methods. With this purpose, we consider a one-coordinate perturbed harmonic oscillator with Hamiltonian $H=p^2/2m+\frac{1}{2}m\omega^2x^2+Ax^3+Bx^4$. The x^3 term does not introduce corrections to the zero-point energy in first order,[37] and the second-order correction is only due to a change in kinetic energy. The x^4 term gives a first-order correction[37] that again is only caused by a kinetic-energy change. Thus, the leading corrections to the zero-point energy due to both perturbing terms originate from changes in the kinetic energy. This is in line with the results presented in Fig. 1, which show that the potential energy derived from PIMC is close to that yielded by the QHA, and the kinetic energy is far from the QHA result. This one-coordinate approach can give us only a very qualitative interpretation of the changes in kinetic and potential energy of the considered crystals with respect to a quasiharmonic approximation. In fact, the whole problem is a many-particle one, in which the lattice vibrations cannot be considered as non-interacting entities when anharmonicities are present. The coupling between vibrational modes obtained in a harmonic or quasiharmonic approximation is expected to increase as the crystal density increases (pressure rises), thus making such approximations less reliable in the description of the vibrational problem.

For what concerns structural and thermodynamic properties of rare-gas solids, the QHA becomes more precise as pressure increases. This is related to the pressure dependence

of the vibrational and elastic energies and is due to two reasons. First, for high pressures the vibrational energy becomes a small part of the internal energy, and hence the influence of lattice vibrations (and of their anharmonicity) on thermodynamic properties will comparatively decrease. The same happens for the free energy F at finite temperatures, since its vibrational part F_{vib} becomes small as compared with the whole F. Thus, for $F_{\mathrm{vib}} \ll F - E_0$, a QHA describes well the pressure dependence of the crystal volume, since it is basically given by the elastic energy of the solid. Second, the intrinsic anharmonicity of the lattice vibrations (as measured by the anharmonicity parameter ξ) decreases as pressure rises (see Fig. 2), and eventually becomes negligible for large P ($\xi \to 0$). Both arguments go in the same direction of making more accurate the QHA.

Nevertheless, the improved accuracy of the QHA as pressure rises is not a particular merit of this approach, since the internal energy becomes dominated by the elastic energy and the actual description of the vibrational modes is not very relevant for thermodynamic properties. It has been also argued[33] that structural properties of solids under pressure can be described rather accurately by a classical model for the lattice vibrations. The origin of this is similar to that described above for the decreasing effect of anharmonicity as P rises, since in this respect the actual description of the lattice vibrations by a classical or a quantum model becomes unimportant for solids under large pressures. This is not necessarily the case for spectroscopic properties of the solids under consideration, because vibrational frequencies predicted by a QHA or by a classical model are not guaranteed to describe correctly the actual ones for high P.

In summary, we have analyzed the influence of a hydrostatic pressure on anharmonic effects of rare-gas solids. Our results indicate that the validity of the QHA to describe structural and thermodynamic properties of these solids increases as pressure is raised. This is mainly a consequence of the relative importance of elastic and vibrational energy, since the latter becomes increasingly irrelevant as pressure rises. Therefore, the precision requirements for a description of the (anharmonic) vibrational modes is reduced with increasing pressure. In the limit of large pressures, even a classical description of these modes can be sufficiently precise to predict several properties of these solids at low temperatures. This is, of course, not the case of vibrational properties, which may require the full quantum treatment with the consideration of zero-point anharmonic effects at high pressures.

We finally note that the extension of the method employed here to study solids under larger pressures, such as those presently reached in experimental studies ($P \sim 100$ GPa), is hampered by the requirement of enlarging enormously the Trotter number (and consequently the CPU time) in PIMC simulations, which has to be increased as the vibrational energy rises. This problem is particularly important to study vibrational properties, since, for very high pressures, thermodynamic properties can be well described by neglecting the quantum nature of the atomic nuclei, as is usually done in electronic-structure calculations.

ACKNOWLEDGMENTS

The authors benefitted from discussions with L. M. Sesé. This work was supported by CICYT (Spain) through Grant No. BFM2003-03372-C03-03.

[1] N. W. Ashcroft and N. D. Mermin, *Solid State Physics* (Saunders College, Philadelphia, 1976).
[2] G. P. Srivastava, *The Physics of Phonons* (Adam Hilger, Bristol, 1990).
[3] G. L. Pollack, Rev. Mod. Phys. **36**, 748 (1964).
[4] M. L. Klein and J. A. Venables, eds., *Rare Gas Solids* (Academic Press, New York, 1976).
[5] R. G. Della Valle and E. Venuti, Phys. Rev. B **58**, 206 (1998).
[6] J. K. Dewhurst, R. Ahuja, S. Li, and B. Johansson, Phys. Rev. Lett. **88**, 075504 (2002).
[7] D. C. Wallace, *Thermodynamics of Crystals* (Wiley, New York, 1972).
[8] N. S. Gillis, N. R. Werthamer, and T. R. Koehler, Phys. Rev. **165**, 951 (1968).
[9] V. V. Goldman, G. K. Horton, and M. L. Klein, J. Low Temp. Phys. **1**, 391 (1969).
[10] M. L. Klein, T. R. Koehler, and R. L. Gray, Phys. Rev. B **7**, 1571 (1973).
[11] A. Paskin, A. M. Llois de Kreiner, K. Shukla, D. O. Welch, and G. J. Dienes, Phys. Rev. B **25**, 1297 (1982).
[12] H. Kleinert, *Path Integrals in Quantum Mechanics, Statistics and Polymer Physics* (World Scientific, Singapore, 1990).
[13] A. Cuccoli, A. Macchi, V. Tognetti, and R. Vaia, Phys. Rev. B **47**, 14923 (1993).
[14] M. Neumann and M. Zoppi, Phys. Rev. B **62**, 41 (2000).
[15] C. Chakravarty, J. Chem. Phys. **116**, 8938 (2002).
[16] M. Neumann and M. Zoppi, Phys. Rev. E **65**, 031203 (2002).
[17] M. H. Müser, P. Nielaba, and K. Binder, Phys. Rev. B **51**, 2723 (1995).
[18] C. P. Herrero, Phys. Rev. B **65**, 014112 (2002).
[19] C. P. Herrero, J. Phys.: Condens. Matter **15**, 475 (2003).
[20] D. N. Timms, R. O. Simmons, and J. Mayers, Phys. Rev. B **67**, 172301 (2003).
[21] A. Cuccoli, A. Macchi, G. Pedrolli, V. Tognetti, and R. Vaia, Phys. Rev. B **56**, 51 (1997).
[22] D. Acocella, G. K. Horton, and E. R. Cowley, Phys. Rev. B **61**, 8753 (2000).
[23] D. Acocella, G. K. Horton, and E. R. Cowley, Phys. Rev. Lett. **74**, 4887 (1995).
[24] M. Grimsditch, P. Loubeyre, and A. Polian, Phys. Rev. B **33**, 7192 (1986).
[25] R. J. Hemley, C. S. Zha, A. P. Jephcoat, H. K. Mao, L. W. Finger, and D. E. Cox, Phys. Rev. B **39**, 11820 (1989).
[26] H. Shimizu, H. Tashiro, T. Kume, and S. Sasaki, Phys. Rev. Lett. **86**, 4568 (2001).
[27] D. Errandonea, B. Schwager, R. Boehler, and M. Ross, Phys. Rev. B **65**, 214110 (2002).
[28] T. Iitaka and T. Ebisuzaki, Phys. Rev. B **65**, 012103 (2001).

[29] T. Tsuchiya and K. Kawamura, J. Chem. Phys. **117**, 5859 (2002).
[30] A. I. Karasevskii and W. B. Holzapfel, Phys. Rev. B **67**, 224301 (2003).
[31] H. M. Lawler, E. K. Chang, and E. L. Shirley, Phys. Rev. B **69**, 174104 (2004).
[32] E. L. Pollock, T. A. Bruce, G. V. Chester, and J. A. Krumhansl, Phys. Rev. B **5**, 4180 (1972).
[33] R. Etters and R. L. Danilowicz, Phys. Rev. A **9**, 1698 (1974).
[34] M. J. Gillan, Philos. Mag. A **58**, 257 (1988).
[35] D. M. Ceperley, Rev. Mod. Phys. **67**, 279 (1995).
[36] J. C. Noya, C. P. Herrero, and R. Ramírez, Phys. Rev. B **53**, 9869 (1996).
[37] L. D. Landau and E. M. Lifshitz, *Statistical Physics*, 3rd ed. (Pergamon, Oxford, 1980).
[38] D. N. Timms, A. C. Evans, M. Boninsegni, D. M. Ceperley, J. Mayers, and R. O. Simmons, J. Phys.: Condens. Matter **8**, 6665 (1996).
[39] C. P. Herrero, Phys. Rev. B **68**, 172104 (2003).
[40] P. Flubacher, A. J. Leadbetter, and J. A. Morrison, Proc. Phys. Soc. London **A78**, 1449 (1961).
[41] E. Somoza and H. Fenichel, Phys. Rev. B **3**, 3434 (1971).
[42] R. J. Hardy, D. J. Lacks, and R. C. Shukla, Phys. Rev. B **57**, 833 (1998).
[43] C. P. Herrero and R. Ramírez, Phys. Rev. B **63**, 024103 (2001).
[44] V. F. Lotrich and K. Szalewicz, Phys. Rev. Lett. **79**, 1301 (1997).
[45] K. T. Tang and J. P. Toennis, J. Chem. Phys. **80**, 3726 (1984).
[46] M. S. Anderson, R. Q. Fugate, and C. A. Swenson, J. Low Temp. Phys. **10**, 345 (1973).
[47] M. S. Anderson and C. A. Swenson, J. Phys. Chem. Solids **36**, 145 (1975).
[48] J. C. Noya, C. P. Herrero, and R. Ramírez, Phys. Rev. B **56**, 237 (1997).
[49] C. P. Herrero, Phys. Status Solidi B **220**, 857 (2000).